frontiers in
NEUROINFORMATICS

Interactive 3D visualization of structural changes in the brain of a person with corticobasal syndrome

Claudia Hänel, Peter Pieperhoff, Bernd Hentschel, Katrin Amunts and Torsten Kuhlen

Journal Name:	Frontiers in Neuroinformatics
ISSN:	1662-5196
Article type:	Methods Article
Received on:	19 Dec 2013
Accepted on:	28 Mar 2014
Provisional PDF published on:	28 Mar 2014
www.frontiersin.org:	www.frontiersin.org
Citation:	Hänel C, Pieperhoff P, Hentschel B, Amunts K and Kuhlen T(2014) Interactive 3D visualization of structural changes in the brain of a person with corticobasal syndrome. *Front. Neuroinform.* 8:42. doi:10.3389/fninf.2014.00042
/Journal/Abstract.aspx?s=752&name=neuroinformatics&ART_DOI=10.3389/fninf.2014.00042:	/Journal/Abstract.aspx?s=752&name=neuroinformatics&ART_DOI=10.3389/fninf.2014.00042
	(If clicking on the link doesn't work, try copying and pasting it into your browser.)

Frontiers in Neuroinformatics

Research Article
24 February 2014

Interactive 3D visualization of structural changes in the brain of a person with corticobasal syndrome

Claudia Hänel [1,*], **Peter Pieperhoff** [2], **Bernd Hentschel** [1], **Katrin Amunts** [2,3] and **Torsten Kuhlen** [1]

[1] *Virtual Reality Group, RWTH Aachen University, Aachen, Germany*
JARA – High Performance Computing
[2] *Institute of Neuroscience and Medicine (INM-1), Research Centre Jülich, Jülich, Germany*
JARA – Translational Brain Medicine
[3] *C. and O. Vogt Institute for Brain Research, Heinrich Heine University Düsseldorf, Düsseldorf, Germany*

Correspondence*:
Claudia Hänel
Virtual Reality Group, RWTH Aachen University, Seffenter Weg 23, Aachen, 52074, Germany, haenel@vr.rwth-aachen.de

ABSTRACT

The visualization of the progression of brain tissue loss, which occurs in neurodegenerative diseases like corticobasal syndrome (CBS), is an important prerequisite to understand the course and the causes of this neurodegenerative disorder. Common workflows for visual analysis are often based on single 2D sections since in 3D visualizations more internally situated structures may be occluded by structures near the surface. The reduction of dimensions from 3D to 2D allows for an holistic view onto internal and external structures, but results in a loss of spatial information. Here, we present an application with two 3D visualization designs to resolve these challenges. First, in addition to the volume changes, the semi-transparent anatomy is displayed with an anatomical section and cortical areas for spatial orientation. Second, the principle of importance-driven volume rendering is adapted to give an unrestricted line-of-sight to relevant structures by means of a frustum-like cutout. To strengthen the benefits of the 3D visualization, we decided to provide the application next to standard desktop environments in immersive virtual environments with stereoscopic viewing as well. This improves the depth perception in general and in particular for the second design. Thus, the application presented in this work allows for an easily comprehensible visual analysis of the extent of brain degeneration and the corresponding affected regions.

Keywords: Volume Rendering, View-dependent Visualization, Virtual Reality, Deformation-based Morphometry, Neurodegeneration, Atrophy

1 INTRODUCTION

Detailed 3D visualizations of the human brain are still challenging with regard to a simultaneous and intuitively graspable representation of the outer surface and internal structures of the brain. The pattern of gyri

and sulci of the outer brain surface provides landmarks for at least coarse localization. Besides, internal brain structures must be distinguishable due to their high functional specificity. Moreover, in neuroscience it is desired to combine such representations with different kinds of additional field data; thresholded maps of such field data shall be integrated with structural data. In the present study, the following types of field data were superimposed on a magnetic resonance tomography (MRT) scan of a person's brain who suffers from the corticobasal syndrome (CBS): Anatomy data, time dependent field data that quantify structural changes on the voxel level, and probabilistic maps of anatomical regions (cf. **Zilles et al.** (2002), **Amunts et al.** (2007)). The structural change data were calculated by analyzing series of longitudinally acquired MRT images by means of a technique called deformation based morphometry (DBM, cf. **Pieperhoff et al.** (2008)). New insights into brain regions that are affected by certain neurodegenerative disease are enabled by exploration of occurring structural changes and its temporal progression.

Visualizations of these brain data by means of 2D sections are widely used, because they are straightforward to implement. However, each of these sections provides only a small cutout of the brain. Thus, it is left to the observer to mentally merge the information into a 3D representation. In particular, it is difficult to relate the information given in a 2D section to the cortical surface of an individual brain. To this end, an additional 3D visualization can be provided separately or in combination with sections. There exist several applications providing side by side 2D and 3D visualizations for brain data. BrainVoyager QX (`http://www.brainvoyager.com/`) is for example a commercial software specialized on functional MRT and diffusion tensor imaging (DTI), but is not easily extendable for other data modalities and their special visualization needs. In comparison to that, OpenWalnut (`http://www.openwalnut.org/`) and MITK (`www.mitk.org`) are open source toolkits that can be extended via plugins, or even within the code basis. Note that OpenWalnut is specialized on DTI data, and MITK is a tool for general medical data that are to be visualized in coronal, sagittal and transversal orientation with an additional 3D visualization.

However, visualizing the human brain in 3D raises its own, distinct challenges that are not considered in particular by those tools. Innovative 3D visualizations have the potential to overcome these shortcomings. A transparent brain surface representation might become difficult to comprehend when the surface is overlapping too many times along the view direction. In contrast, the visualization as an opaque surface will occlude major parts of itself. **Thompson et al.** (2007) and **Zhou et al.** (2013) use opaque surface renderings of the whole brain or of certain segmented structures that are colored by additional field data, such as volume change data or statistical scores. Thus, any information inside or outside the rendered surfaces is discarded. To enable the representation of subcortical brain structures like the border between cortex and white matter, subcortical nuclei, or ventricles, 3D visualizations are often combined with up to three clipping planes (cf. **Olabi et al.** (2012); **Weber et al.** (2008)). These planes define a clipping cuboid, in which the part of the brain inside this cuboid is removed and the clipping planes itself represent 2D sections. In case of combined data modalities in one visualization, clipping can be limited to individual data sets as shown in **Born et al.** (2009) and **Rieder et al.** (2013), where only the anatomy inside the clipping cuboid is removed and fiber bundles stay visible. Additionally, a transparent representation of the brain in the cutout improves spatial perception of non-clipped structures.

Using a cuboid for the clipping, however, may require clipping too large parts of the brain, for example, when structures in the central part of the brain should be depicted. Therefore, a more flexible clipping geometry would be beneficial. As an alternative to the clipping planes, **Rick et al.** (2011) present a flashlight metaphor that enables the user to manually create a cutout into the opaque anatomy volume visualization by interactively changing the diameter and depth of a clipping cone. Still, this method is of limited use for elongated structures when observing the whole structure at once, because the diameter of the cone becomes unnecessarily large for the non-elongated direction and again too large parts of the brain might be clipped. Otherwise, a cone with a small diameter could be moved manually through the volume showing only a small part of the volume of interest (VOI) at once.

More data-driven visualization concepts are presented, e.g., by **Hauser et al.** (2001), **Krüger et al.** (2006), **Bruckner et al.** (2006), and **Viola et al.** (2004). These designs have in common that they locally decrease the opacity of occluding structures to show internal ones. **Hauser et al.** (2001) suggest to render

different structures of a data set as individual objects separately in a first step. These objects are merged in a second step in order to give each of them a customized appearance in the final visualization. To focus on a small part of the whole volume, **Krüger et al.** (2006) use focus and context techniques and apply different weights, transparency functions, or color properties for focus and context objects. **Bruckner et al.** (2006) motivate their concept by hand-drawn illustration techniques and influence the focus mainly by defining the distance to the eye point and a gradient magnitude. The user can influence the sharpness of transition between clipped and visible structures, and the depth of clipping. The drawback of the three previously described techniques is the missing depth information for the VOI. **Viola et al.** (2004) resolve this problem with a technique using a conical cutout, that is comparable to the flashlight metaphor of **Rick et al.** (2011) and shows anatomical information on its faces, thus giving depth information. This importance-driven volume rendering (IDVR) approach has the advantage that the cutout can be assigned to a particular structure, whereby it automatically adjusts to the VOI's size. Furthermore, the cutout follows the view direction of the user and therefore stays always perfectly aligned. But for neuroscientific applications this technique might be further improved by providing additional information at the same depth as the VOI creating a section-like view onto the data and a data-depended clipping object for the deformation data.

Based on the previous findings we present in this work two designs for the visualization of brain data with structural changes. The user interface of our visualization system had to enable an intuitive interaction and to provide both, an overview of the whole data and a detailed view of spatial relations. Therefore, the first design allows for a good overview by means of a transparent anatomy and an interactively alignable section to derive detailed anatomical information (cf. **Figure 1**). The second design extends the approach of **Viola et al.** (2004) by using a frustum of a cone as clipping object (cf. **Figure 2**) to provide more context information about nearby structures on the clipping planes (cf. **Figure 3**).

The rest of the paper is structured as follows: In section 2 we go, after a more detailed description of our data base, into detail with our visualization designs and interaction concept. Section 3 discusses the benefits of our implementation and in section 4 we draw a conclusion and give an outlook onto possible future improvements.

2 METHODS

Before we describe the two visualization designs mentioned above in detail, the underlying data modalities are clarified. Furthermore, we show how the user interface of our visualization system aims for an intuitive interaction and provide both, an overview of the whole data and a detailed view of spatial relations.

2.1 DATA AND IMAGE ANALYSIS

The MRT data that were examined exemplary in the scope of this work are from one person, and had been acquired by **Südmeyer et al.** (2012) within a longitudinal study of aging and neurodegenerative diseases. A series of T1-weighted MRT images of one subject with a voxel-size of $1 \times 1 \times 1\,mm^3$ was used to visualize the brain structure. These images were acquired at five points in time within a total interval of 26 month. The initial MRT image was segmented by deleting the value of every voxel not belonging to brain tissue. Segmentation masks were automatically generated by a procedure which was implemented in the program SPM (`http://www.fil.ion.ucl.ac.uk/spm/`) and afterwards manually corrected. Maps of volume changes, which were superimposed to the structural image, were calculated by DBM in the following way. Each follow-up MRT image of the subject was non-linearly registered with the initial image by minimizing the voxel-wise squared intensity differences between both images, regularized by an elastic energy term which penalized non-biological distortions. The image registration yielded for each follow-up MRT image a deformation field that assigned to each voxel of the initial MRT image a vector that pointed to the corresponding position in the follow-up image. From this deformation field, a map of voxel-wise relative volume differences was derived. Further details of this analysis can be found

in **Pieperhoff et al.** (2008). In order to visualize the temporal evolution of tissue degeneration fluently, volume change maps in-between the actual time points–month 0, 16, 20, 23, and 26–were interpolated to a total number of 27 data sets.

Maps of anatomical regions used here originate from the JuBrain Cytoarchitectonic Atlas (`https://www.jubrain.fz-juelich.de`). They were gained by cytoarchitectonical based parcellations in histological sections of post-mortem brains (cf. **Zilles et al.** (2002); **Amunts et al.** (2007)).

The anatomical data, time dependent field data and cortical areas were used to develop the visualization designs presented below and were a use case to examine the supportive effect in the visual analysis of these data.

2.2 VISUALIZATION

We developed two different visualization designs to support the spatial understanding of the data. The first design used a transparent 3D representation of the anatomy and an opaque section. The second design was based on the IDVR algorithm as described in **Viola et al.** (2004) creating a view-dependent cutout around a defined VOI. In both designs, the degeneration of the brain tissue was visualized by means of time varying data, which were mapped to a red to yellow color map, with red meaning small and yellow large volume decline (cf. **Südmeyer et al.** (2012)). Additionally, to draw conclusions from affected tissue to brain structures, selected cortical areas were provided as defined in the JuBrain atlas. For the visualization design described below, we had have to follow the requirement to present internal structural information with respect to external anatomy in a meaningful way. The use of volume rendering and an interactive adjustment of opacity values for each data set facilitated, for example, a visualization of structural changes caused by tissue atrophy and anatomical regions. Furthermore, the combined ray casting for all data in one volume renderer enabled a correct depth perception. Based on this, our first visualization design combined common modalities and was used particularly as an overview visualization, whereas the second design allowed for a detailed examination of a selective VOI.

Overview Design

Sections are a standard tool of neuroscientists for 2D brain visualization making a systematic analysis possible without occluding any information. They can be combined with 3D visualizations when using them as clipping planes (cf. **Cabral et al.** (1994); **Rößler et al.** (2006); **Rick et al.** (2011)) to assist spatial orientation. Our proposed overview design built upon this idea by showing the brain anatomy semi-transparently by the use of volume rendering and an additional 2D section of the original MRT data. Thus both, the complex structure of the brain surface with gyri and sulci as well as internal regions remained visible, and no information in front of the section was lost as with clipping planes. To give an overview on the tissue degeneration, the deformation data were blended into the 3D anatomy volume. The final design can be seen in **Figure 1**.

Importance-Driven Volume Rendering Design (IDVR Design)

In comparison to the overview design, the IDVR design was a more specialized view for a detailed examination of specific brain areas. The anatomy was visualized in an opaque fashion and a cutout facilitated a view into the volume by removing only as much anatomy as necessary and staying automatically aligned to the user's view direction. Therefore, the design used an advanced algorithm based on **Viola et al.** (2004), and specified a VOI that is always visible due to a view-dependent cutout. The original work defines a conical cutout, with the tip of the cone being determined by the VOI's deepest voxel along the view direction. The faces of the cone help to determine the depth of the VOI in the overall volume. Still, nearby structures at the same depth of the VOI may be covered by the surrounding brain tissue. Therefore, it is more favorable for applications in neuroscience to expand the cutout by using a section-like plane that is aligned along the rear side of the VOI. Thus, as a first simple extension to Viola's algorithm the tip

of the cone was moved backwards and the top plane of a frustum was created at the level of the deepest VOI voxel. In our case, the VOI was defined by a neuroanatomical region, which often has a complex structure, such that its depth texture is strongly varying. Hence, creating the section only on basis of one depth value would neglect nearby structures on all other depth levels of the VOI. Therefore, we adapted the algorithm to define the top surface of a frustum-like cutout with a section that is approximated using all values of the VOI's backface (cf. **Figure 2**).

The cutout calculation was based on multi-pass raycast rendering and worked as follows. In the first pass, a special modification of a depth texture of the VOI was defined as not only the depth values are interesting, but also the exact sample position in the volume. Therefore, rays were directed into the volume that were defined by a previously calculated ray entry points texture T_R and a ray exit point texture T_E. Along each ray, the x-, y-, and z-coordinate of the deepest VOI voxel and the accumulated length l_a until this point were determined. These values were stored into the output texture T_V of this first rendering pass. If the ray did not hit the VOI at all, the four texel values were set to zero.

In the second rendering pass, the cutout was defined. To find the best definition of the top surface of the frustum with respect to the best information retrieval and smoothness, three different implementations were tested. The first two approaches of the top surface definition varied only in the determination of the texel $P_V \in T_V$ that is used as reference point for further calculations (cf. **Figure 4 left, middle**). In the first case a vector $\overrightarrow{P_R P_{V_1}}$ was sought, where $P_R \in T_R$ was the current ray entry point and $P_{V_1} \in T_V$ is defined by the closest texel of T_V with $l_a > 0$, within a maximum distance d in X- and Y-direction of T_V. Therefore, the algorithm iterated over all texels of T_V from $-d$ to $+d$ distance in X- and Y-direction starting from the texel with the same texel coordinates as P_R.

In the second case, we adapted this iteration step by not minimizing $|\overrightarrow{P_R P_{V_1}}|$, but rather find the texel $P_{V_2} \in T_V$ that created a vector $\overrightarrow{P_R P_{V_2}}$ with a minimum angle between $\overrightarrow{P_R P_{V_2}}$ and the X- or Y-axis. The iteration starts at 0, checks in $\pm d$ in X- and Y-direction, and terminates if a sufficient P_{V_2} is found. From this point on, the calculations were identical for the first and second implementation and we defined $P_V = P_{V_1}$ or $P_V = P_{V_2}$, respectively.

Let r_1 be the maximum length of $\overrightarrow{P_R P_V}$, with

$$r_1 = \sqrt{d^2 + d^2}, \text{ where } \sqrt{d^2 + d^2} \geq |\overrightarrow{P_R P_V}|. \tag{1}$$

If $\overrightarrow{P_R P_V}$ existed, it was possible to determine a vector $\overrightarrow{RV}$, with V being the corresponding voxel of the VOI to P_V saved in the output texture of the first rendering pass T_V, and R being defined with the help of the congruence theorem of triangles, where an edge with an angle of 90° could be constructed from the view ray to V (cf. **Figure 5**). If $|\overrightarrow{RV}|$ was within a radius r_2, with $r_2 \leq r_1$, the ray hit the top surface of the frustum and the depth value c of the cutout for the current view ray was set to the depth value of V. Otherwise, the cutout depth c was calculated as follows

$$c = |\overrightarrow{RV}| - \frac{|\overrightarrow{P_R P_V}| - r_2}{r_1 - r_2}. \tag{2}$$

The result of the first approach showed circular artifacts around small parts of the VOI that stuck out, and where depth changes of the VOI occurred (cf. **Figure 6 left**). For the second approach, we see hard edges in diagonal orientation (cf. **Figure 6 middle**). To create a smoother frustum top surface, neglecting small outliers, we implemented a third approach which is schematically shown in **Figure 4 right**. In addition to P_{V_1} the texel P_{V_d} in T_V was sought within a maximum distance $\pm d$ to P_R in X- and Y- direction with the highest l_a value. $\overrightarrow{P_R P_V}$ was calculated as in the previous approaches, but $\overrightarrow{RV}$ was replaced with $\overrightarrow{RV_d}$ and

the additional depth had to be included in the calculation of the frustum faces, resulting in

$$c = |\overrightarrow{RV_d}| - |\overrightarrow{RV_d}| \cdot \frac{\left(|\overrightarrow{P_R P_V}| - r_2\right)}{r_1 - r_2}. \tag{3}$$

Although the depth value of the top surface is determined by the depth value of V_d, $|\overrightarrow{RV}|$ still defines whether the view ray hits the top surface or is part of a frustum face. An exemplary smoothed cutout can be seen in **Figure 6 right**.

2.3 INTERACTION

Depth perception can be improved by rotating, panning, and zooming (cf. **Swanston and Gogel** (1986)), and therefore interaction with the brain model in the 3D visualization became necessary. In immersive virtual environments, correct depth relations can already be perceived without additional conscious interaction. Therefore, we provided the application for both, standard desktop setups and 3D immersive virtual environments with stereoscopic vision. To this end, we used the open source, cross-platform ViSTA toolkit (cf. **Assenmacher and Kuhlen** (2008)) for easy scalability to different systems. In the immersive setup, the depth impression of the cutout in the IDVR design got more comprehensible and it was clearly visible where the border between faces and top surface of the frustum was. The advantage of virtual environments over 2D displays for depth perception and estimation were shown several times, e.g., in **Armbrüster et al.** (2006) and **Naceri et al.** (2010) and in particularly for volume rendered data in **Laha et al.** (2012).

As we provided the application for Virtual Reality setups, an alternative to the classical 2D menu interaction became necessary. To this end, we decided to use extended pie menus as described by **Gebhardt et al.** (2013). They scale to 2D and 3D environments and can interactively be moved in the scene while staying aligned to the user's orientation. The menu is hierarchically arranged and can be divided into various submenus (cf. **Figure 3**). Aside from changing the view perspective onto the data, all possible interactions were controlled via these menus. The most important ones are explained below.

Time Navigation–This submenu held the time navigation, where the user was able to set the animation speed or can manually step through all time steps of the presented data.

Cortical Areas–It was possible to select predefined cortical areas in this submenu that were to be visualized. Prior to launching the program, the user was able to group and color-cod these areas in a separate settings file These definitions were also represented in the pie menu, allowing the user to hide or display whole area groups with a single mouse click. Furthermore, the opacity can be adjusted to provide a view onto degeneration occurring inside of the cortical area.

Importance Driven Volume Rendering–Here the user can switch to the IDVR design. Depending on the available data sets of the subject, a variety of options existed. By default the VOI was defined by the visible cortical area(s). If provided the user was able to select any other VOI defined by field data as well. It can be useful to show other data next to the VOI in the cutout. Therefore, the user might choose to visualize the degeneration, or if provided, any other data exempt from the anatomy.

Color Map–This submenu allowed users to adapt the opacity and enhance the contrast of the anatomy. As the prototype should be applicable for different data sets, these values had to be changed manually as the acquired volumes of different people can vary in their gray value distribution. Furthermore, the color menu allowed users to change the threshold for the deformation values to exclude small degeneration values and set the focus on larger ones. The adjustability of the opacity for these values led to a good spatial orientation particularly in the IDVR design as the degeneration could be visualized in the cutout and a high transparency preserves a good view onto the cutout faces. Moreover, in the overview design the right balance between opacity of cortical areas and degeneration allowed for good visual comparability of relationship between the two volumes.

3 RESULTS AND DISCUSSION

According to the informal feedback from a number of domain experts, the visualization of anatomical structure and superimposed field data by volume rendering enables neuroscientists to observe the data described in section 2.1 not only on the surface but also inside the brain. This is an advantage over surface reconstruction based visualization, because the latter is typically limited to field data on or near the surface, which causes a great loss of information. In studies of neurodegenerative diseases, it makes an important difference if the tissue atrophy that is quantified by the superimposed volume change data occurs only in the cortex, or if also subcortical regions and white matter (i.e. fibers deep inside the brain which connect brain regions) are affected. For instance, the data examined here show a progressive atrophy, which includes both the motor cortex areas and the pyramidal tract. But transparent volume rendering of the brain often yields diffuse borders, whereas in surface based visualization the perception of the surface shape can be enhanced, for example, by the simulated effects of lighting, reflection, and shadows. Moreover, brain structures that are deep inside the brain and have only low contrast to their environment are hardly perceived when volume rendering of an MRT image is used exclusively.

Therefore, a 2D section is added in the overview design onto which the voxel values of the structural image of the brain are mapped, such that cortex, subcortical nuclei, and white matter are better distinguishable. The brain in front of the added plane is not removed and thus landmarks for an anatomical localization are still provided. This design is particularly useful, when certain features near or within the brain cortex like the atrophy of certain gyri shall be shown.

However, in the IDVR design the brain in front of the clipping surface is removed, whereas the anatomical maps and the volume change data are still completely rendered. This design is more appropriate to show deeper parts of the brain: By means of the anatomical regions in front of the clipping surface and the surface texture, a good localization is possible. In particular, the overlap of anatomical regions and volume change data is intuitively displayed by the blending of their colors (cf. **Figure 7**).

Moreover, the automatic alignment of the clipping surface when the brain is moved relative to the observer enables a simple interaction, which gives a good spatial perception even in non-virtual environments. The extent of the removed part of the brain can be controlled by the selection of predefined anatomical regions and additional parameters like the aperture of the frustum. We observed that using the application in a user-friendly immersive virtual environment enhances the perception of the spatial relations, in particular of spatial depth.

Since this application is to be used interactively, the frame rate is an important performance issue to be investigated in more detail. In comparison to visualizations of geometries, volume rendering approaches lag in performance, and in addition the use of stereo viewing in an immersive virtual environment halves the frame rate due to the generation of two simultaneous images (one per eye). We tested our application on two systems: The first is used as desktop environment, and runs Windows 7 on Intel Xeon CPU E5540 with four cores at 2.5GHz, an Nvidia GeForce GTX 480 graphics card, and 12GB RAM; the second system is used as virtual environment with a passive stereo system, head tracking, and runs Windows 7 on Intel Xeon CPU E5530 with four cores at 2.4 GHz, but with an Nvidia Quadro 6000 graphics card, and 4GB of RAM. With a resolution of 1400×1050 we achieve for the overview design about 30 fps in stereo mode which fulfills the requirement for interactivity. The implementation of the IDVR design is based on the same volume renderer, thus a higher frame rate cannot be expected. We are limited by the iteration over all neighboring texels when seeking P_V as it cannot be early terminated, because there is always the possibility to find a closer V respectively a V_d with higher l_a. To solve this problem, we introduced a parameter to the IDVR calculation to set the accuracy in the iteration. Under assumption of a sufficiently large texture resolution of T_V, every i-th texel can be skipped and is not tested to be a candidate for V or V_d. The value for i can be changed via the pie menu. For $i = 2$ nearly no visual artifacts can be found. For $i = 3$ noticeable impacts in form of loose wrong depth values appear, but this method is still reasonable allowing for better performance and the artifacts are not disturbing the overall depth perception in the cutout. The achieved frame rates (cf. **Table 1**) for a scene comparable to the one shown in **Figure 3** show that also the IDVR design can be used interactively in virtual environments, but clearly

Table 1. Results of performance tests of the visualization designs (averaged values from different view points), the overview design with common volume rendering and the IDVR design with different precision states for the cutout generation.

	Nvidia GeForce GTX 480 (mono view)	**Nvidia Quadro 6000 (stereo view)**
Overview Design	55 fps	30 fps
IDVR Design		
$i = 1$	4 fps	3 fps
$i = 2$	11 fps	7 fps
$i = 3$	18 fps	10 fps

still needs performance improvements. However, in general the frame rate of our application is highly dependent on the window size, the size of the volume on the screen, and for the IDVR design on the value of distance d.

4 CONCLUSION AND FUTURE WORK

In this paper, we have presented two visualization designs to address the challenge of depicting complex 3D information of brain data. While the first approach provides an overview of the data, the second allows for a more detailed examination and supports the visual analysis as described in the results section. Even if current work as **Laha et al.** (2012) shows that the visualization in virtual environments supports the analysis of volume data, a future work would be to generalize this first user feedback to our application in an expert review. First, the general improvement of spatial impression and the ability of correct spatial localization with our designs in comparison to commonly used 2D section views should be proven, for example, by determining the extension of an artificial tissue degeneration and its spatial localization. Second, this experiment should be repeated in an immersive virtual environment and then compared to the results of desktop environments. More important than this quantitative is a qualitative analysis. Since our application is supposed to benefit the daily workflow of neuroscientists, their expert impression of additional or more easily grasped information should be gathered.

Illustrations in anatomical text books like **Nieuwenhuys et al.** (2008) are excellent artworks that selectively emphasize certain structural entities or parts of the brain while showing the surrounding brain structure. These figures were artistic drawings, but it is desirable to achieve similar presentations by computerized 3D visualizations which can be manipulated by user interaction (cf. **Bruckner et al.** (2006)). In particular, the gradient based emphasis of surface structures could be used to stress the brain surface and show the ventricles in the overview design more clearly. Furthermore, an enhanced contrast-to-noise ratio of the MRT data and a visual smoothing would improve the quality of the visualization and allow for easier analysis. As discussed in section 3, the IDVR design could benefit from a faster cutout calculation to ensure a higher frame rate which in turn would lead to increased interactivity. Therefore, one approach might be to use distance maps created from the result of the first rendering pass and discard the iteration approach during the second rendering pass that is mainly responsible for the frame rate decrease.

In conclusion, an initial feedback of domain experts for our two visualization designs has already shown to improve the spatial localization of brain structures affected by CBS and the understanding of its temporal progression which motivates further research.

ACKNOWLEDGEMENT

Funding: Helmholtz Portfolio Theme "Supercomputing and Modeling for the Human Brain" and partially by the "Human Brain Project" as part of the FET Flagship Programme.

REFERENCES

Amunts, K., Schleicher, A., and Zilles, K. (2007), Cytoarchitecture of the cerebral cortex–More than localization , *NeuroImage*, 37, 4, 1061–1065, doi:10.1016/j.neuroimage.2007.02.037

Armbrüster, C., Wolter, M., Valvoda, J. T., Kuhlen, T., Spijkers, W., and Fimm, B. (2006), Virtual Reality as a Research Tool in Neuropsychology: Depth Estimations in the Peripersonal Space, *CyberPsychology & Behavior*, 9, 6, 654

Assenmacher, I. and Kuhlen, T. (2008), The ViSTA Virtual Reality Toolkit, in Proceedings of the IEEE VR 2008 Workshop Software Engineering and Architectures for Realtime Interactive Systems (SEARIS) (Shaker Verlag), 23–28

Born, S., Jainek, W., Hlawitschka, M., Scheuermann, G., Tantakis, C., Meixensberger, J., et al. (2009), Multimodal Visualization of DTI and fMRI Data Using Illustrative Methods, in Bildverarbeitung für die Medizin 2009, Springer (Springer), 6–10, doi:10.1007/978-3-540-93860-6_2

Bruckner, S., Grimm, S., Kanitsar, A., and Gröller, M. E. (2006), Illustrative Context-Preserving Exploration of Volume Data, *IEEE Transactions on Visualization and Computer Graphics*, 12, 6, 1559–1569

Cabral, B., Cam, N., and Foran, J. (1994), Accelerated Volume Rendering and Tomographic Reconstruction Using Texture Mapping Hardware, in Proceedings of the 1994 symposium on Volume visualization (ACM), VVS '94, 91–98, doi:10.1145/197938.197972

Gebhardt, S., Pick, S., Leithold, F., Hentschel, B., and Kuhlen, T. (2013), Extended Pie Menus for Immersive Virtual Environments, *IEEE Transactions on Visualization and Computer Graphics*, 19, 4, 644–651, doi:10.1109/TVCG.2013.31.

Hauser, H., Mroz, L., Bischi, G. I., and Gröller, M. E. (2001), Two-level volume rendering, *IEEE Transactions on Visualization and Computer Graphics*, 7, 3, 242–252, doi:10.1109/2945.942692

Krüger, J., Schneider, J., and Westermann, R. (2006), ClearView: An Interactive Context Preserving Hotspot Visualization Technique, *IEEE Transactions on Visualization and Computer Graphics*, 12, 5, 941–948, doi:10.1109/TVCG.2006.124

Laha, B., Sensharma, K., Schiffbauer, J., and Bowman, D. (2012), Effects of Immersion on Visual Analysis of Volume Data, *IEEE Transactions on Visualization and Computer Graphics*, 18, 4, 597–606, doi:10.1109/TVCG.2012.42

Naceri, A., Chellali, R., Dionnet, F., and Toma, S. (2010), Depth perception within virtual environments: Comparison between two display technologies, *International Journal On Advances in Intelligent Systems*, 3, 1 and 2, 51–64

Nieuwenhuys, R., Voogd, J., and van Huijzen, C. (2008), The Human Central Nervous System (Springer-Verlag, Berlin), 4th edition

Olabi, B., Ellison-Wright, I., Bullmore, E., and Lawrie, S. (2012), Structural brain changes in first episode Schizophrenia compared with Fronto-Temporal Lobar Degeneration: a meta-analysis, *BMC Psychiatry*, 12, 1, 1–13, doi:10.1186/1471-244X-12-104

Pieperhoff, P., Südmeyer, M., Hömke, L., Zilles, K., Schnitzler, A., and Amunts, K. (2008), Detection of structural changes of the human brain in longitudinally acquired MR images by deformation field morphometry: Methodological analysis, validation and application, *NeuroImage*, 43, 2, 269 – 287, doi:10.1016/j.neuroimage.2008.07.031

Rick, T., von Kapri, A., Caspers, S., Amunts, K., Zilles, K., and Kuhlen, T. (2011), Visualization of Probabilistic Fiber Tracts in Virtual Reality, *Studies in Health Technology and Informatics*, 163, 486–492, doi:10.3233/978-1-60750-706-2-486

Rieder, C., Brachmann, C., Hofmann, B., Klein, J., Khn, A., Ojdanic, D., et al. (2013), Interactive Visualization of Neuroanatomical Data for a Hands-On Multimedia Exhibit, in L. Linsen, H. C. Hege,

and B. Hamann, eds., Visualization in Medicine and Life Sciences (Eurographics Association), 37–41, doi:10.2312/PE.VMLS.VMLS2013.037-041

Rößler, F., Tejada, E., Fangmeier, T., Ertl, T., and Knauff, M. (2006), GPU-based Multi-Volume Rendering for the Visualization of Functional Brain Images, in Proceedings of SIMVIS '06 (Publishing House), 305–318

Südmeyer, M., Pieperhoff, P., Ferrea, S., Krause, H., Groiss, S., Elben, S., et al. (2012), Longitudinal Deformation-Based Morphometry Reveals Spatio-Temporal Dynamics of Brain Volume Changes in Patients with Corticobasal Syndrome, *PLoS one*, 7, e41873, doi:10.1371/journal.pone.0041873

Swanston, M. T. and Gogel, W. C. (1986), Perceived size and motion in depth from optical expansion, *Attention, Perception, & Psychophysics*, 39, 5, 309–326

Thompson, P. M., Hayashi, K. M., Dutton, R. A., Chiang, M.-C., Leow, A. D., Sowell, E. R., et al. (2007), Tracking Alzheimer's Disease, *Annals of the New York Academy of Sciences*, 1097, 1, 183–214, doi:10.1196%2Fannals.1379.017

Viola, I., Kanitsar, A., and Gröller, M. E. (2004), Importance-Driven Volume Rendering, in Proceedings of IEEE Visualization '04, 139–145

Weber, S., Habel, U., Amunts, K., and Schneider, F. (2008), Structural Brain Abnormalities in Psychopaths - a Review, *Behavioral Sciences and the Law*, 26, 7–28, doi:10.1002/bsl.802

Zhou, Y., Kierans, A., Kenul, D., Ge, Y., Rath, J., Reaume, J., et al. (2013), Mild Traumatic Brain Injury: Longitudinal Regional Brain Volume Changes, *Radiology*, 267, 3, 880–890, doi:10.1148/radiol.13122542

Zilles, K., Schleicher, A., Palomero-Gallagher, N., and Amunts, K. (2002), Quantitative analysis of cyto- and receptor architecture of the human brain (Elsevier), chapter 21, 2nd edition, 573–602

FIGURES

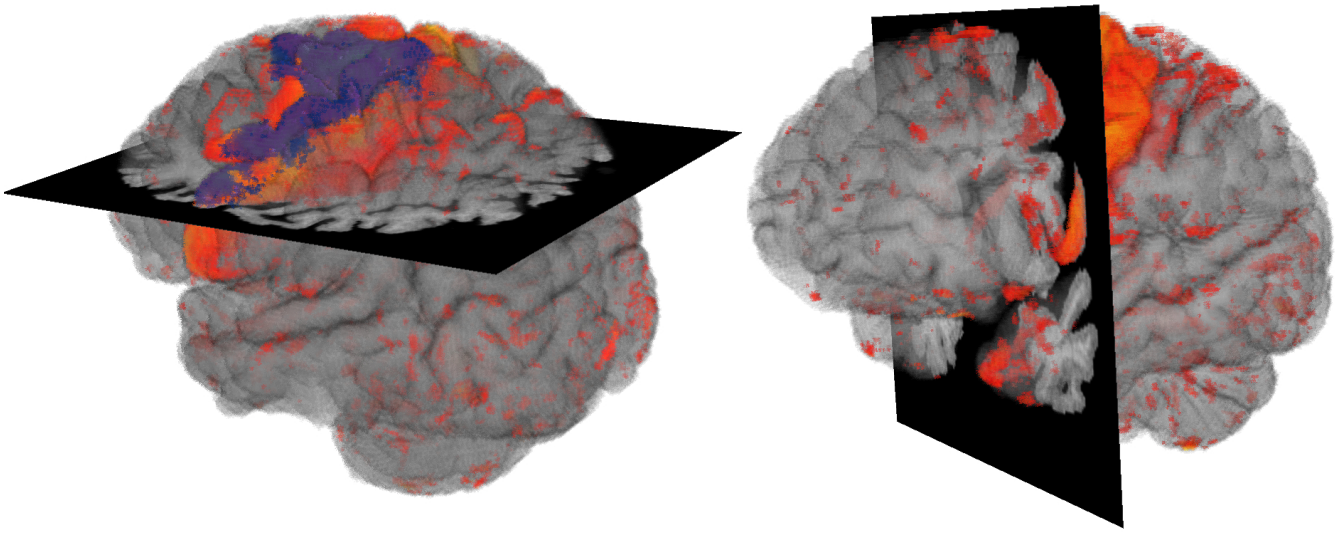

Figure 1. Overview Design: Volume visualization showing brain degeneration (yellow/red) and the premotor cortex area (blue) in anatomical context (gray).

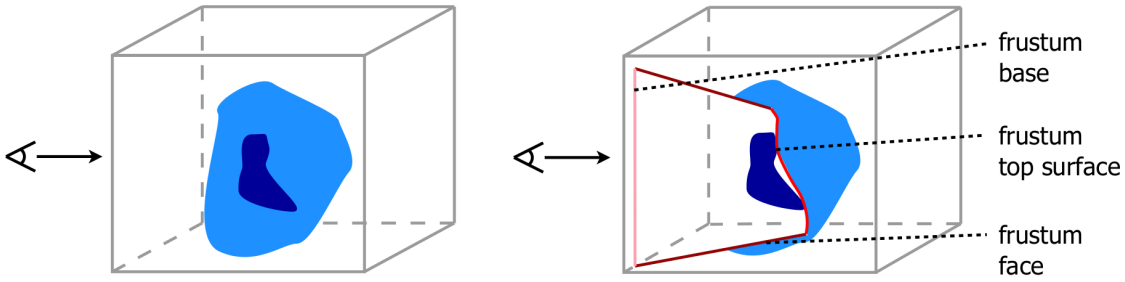

Figure 2. View dependent frustum-like cutout into the volume (light blue) following the depth structure of the VOI (dark blue).

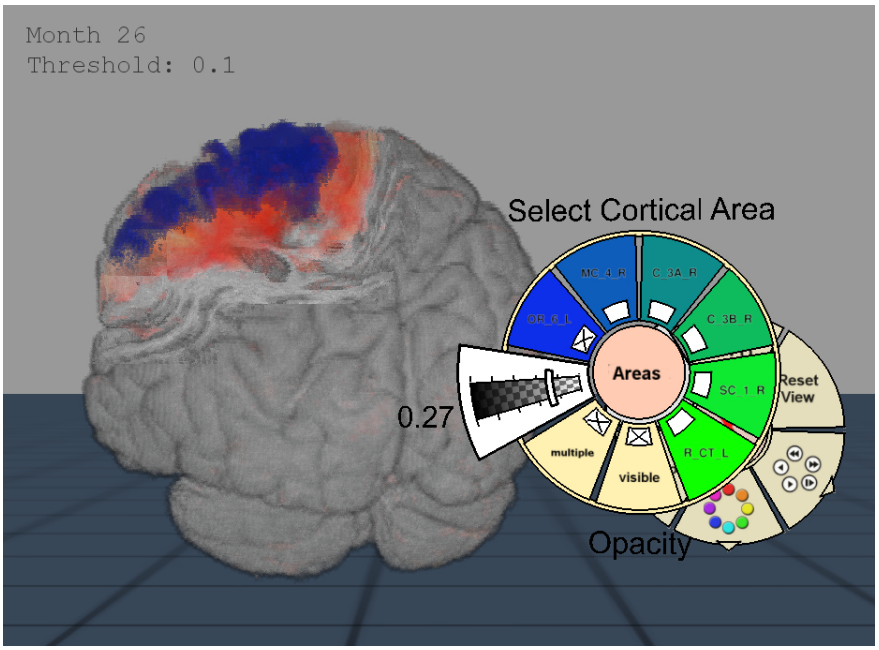

Figure 3. Importance-Driven Volume Rendering Design: A view-dependent cutout is created to the premotor cortex area (blue). Furthermore, this screenshot shows the application when changing the opacity of the cortical area via pie menu.

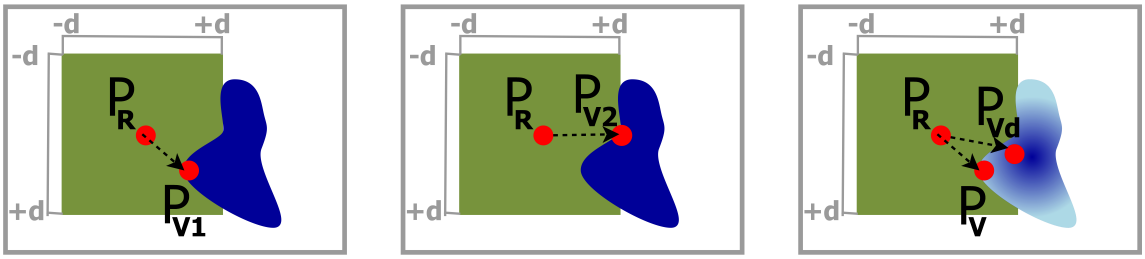

Figure 4. Determination of the local depth value in the cutout. Left: Use depth of P_{V_1} as the closest texel of the VOI's depth texture to the ray entry point P_R. Middle: P_{V_2} is the most straight aligned texel in relation to P_R. Right: A darker color in the VOI depicts a higher depth value. P_V is the closest texel to P_R and is used to calculate the distance to the VOI, but P_{V_d} has the highest depth value in distance d around P_R, and is utilized as depth value.

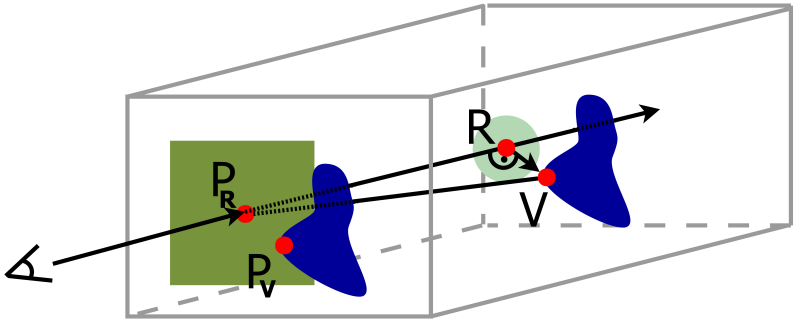

Figure 5. Schematic illustration of the construction from the closest depth point of the volume of interest V onto the view ray R. In dark blue we see in the back the volume of interest and its projected depth texture on the near clipping plane. The dark green area limits our search area from the ray entry point P_R to a nearby VOI point P_V, and the light green circle with radius r_2 limits the top surface size.

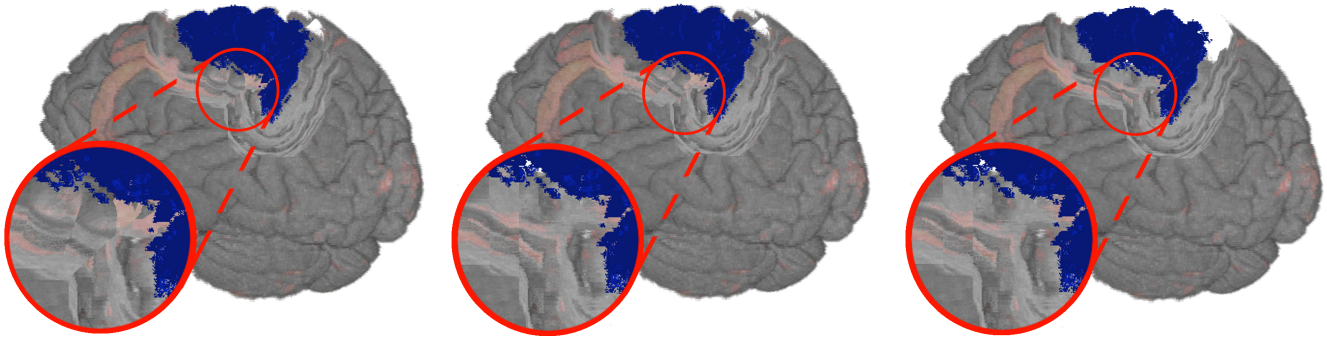

Figure 6. Clipping artifacts depend on the definition of the distance value and are clearly visible when observing transitions in the sulci (dark gray) in the detail view. Left: Circular artifacts when using the closest voxel of the VOI. Middle: Diagonal artifacts when preferring voxels in straight alignment. Right: Smoothest result with homogeneous depth values for a nearby voxel.

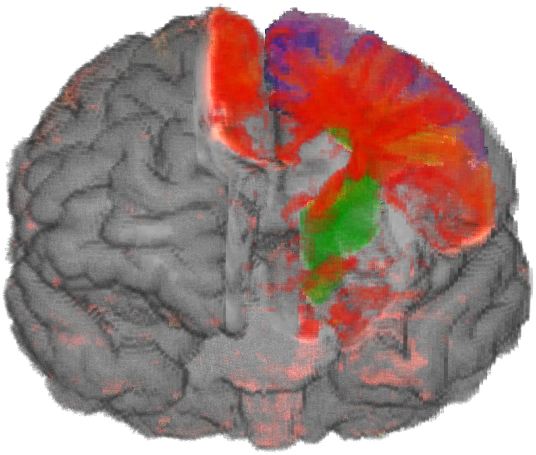

Figure 7. Atrophic part of the brain (red to yellow) of a person with CBS and maps of anatomical regions (blue premotor cortex, green cortico-spinal tract). The removed part of the brain is adjusted to the selected anatomical regions. The overlap between atrophic parts and anatomical regions can be recognized by the blending of different colors.

Figure 1.JPEG

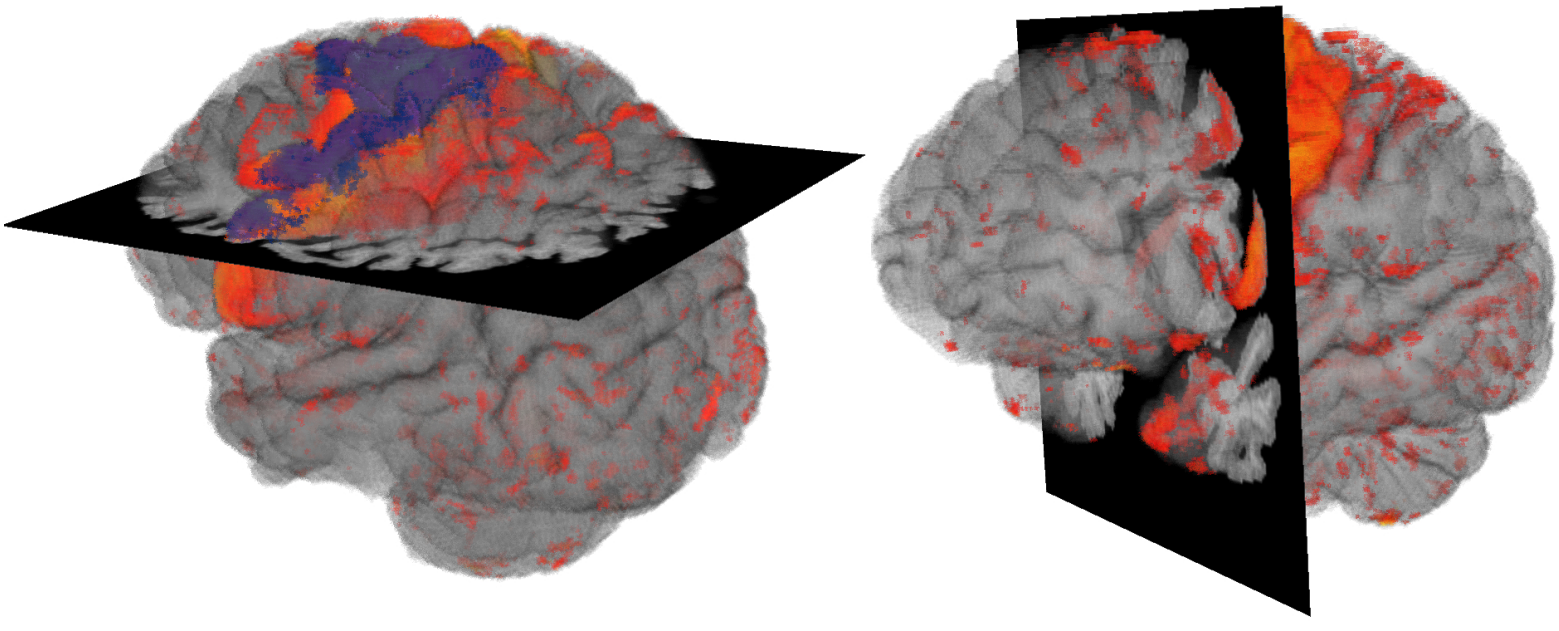

Figure 2.JPEG

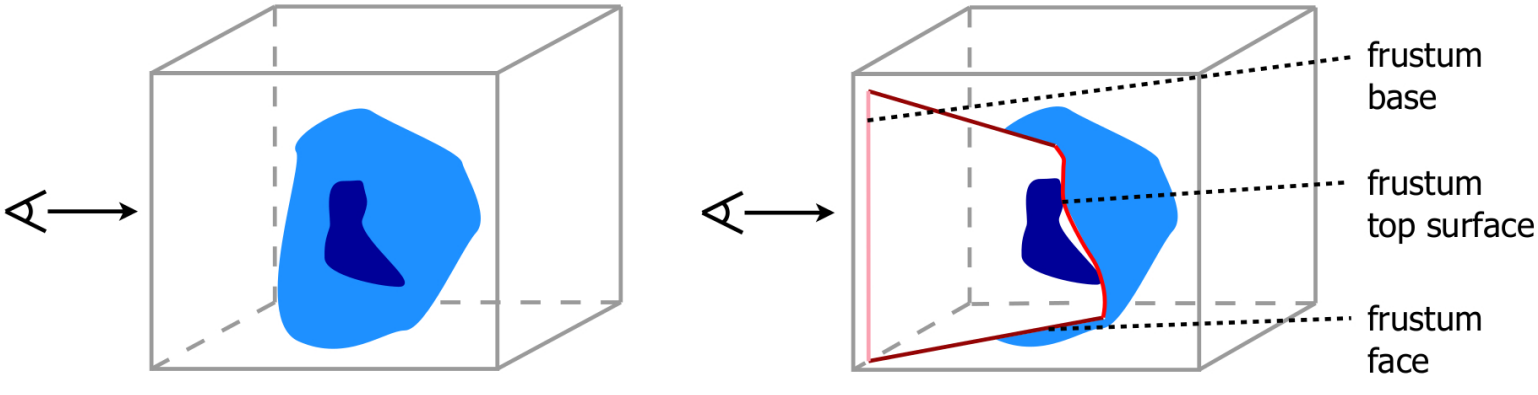

Figure 3.JPEG

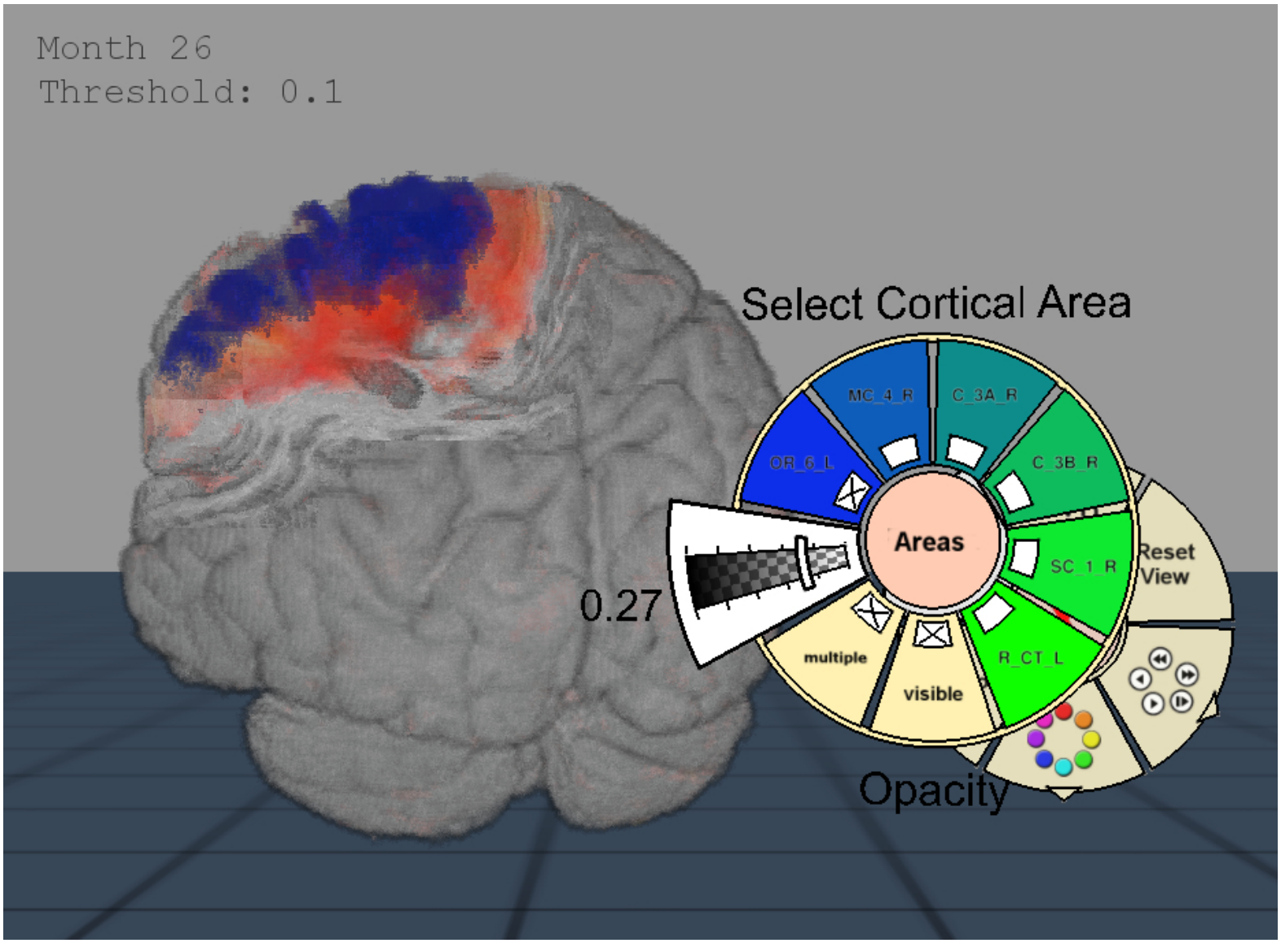

Figure 4.JPEG

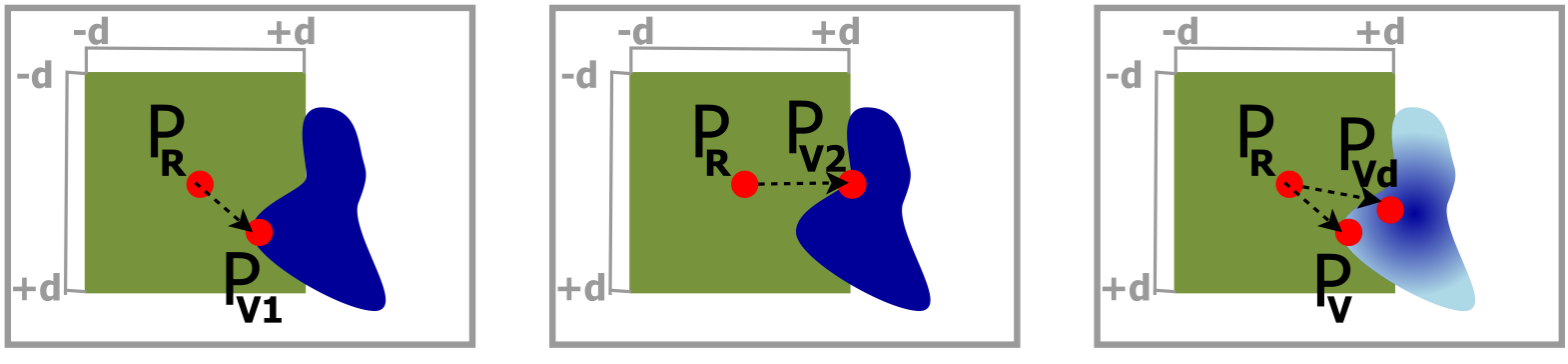

Figure 5.JPEG

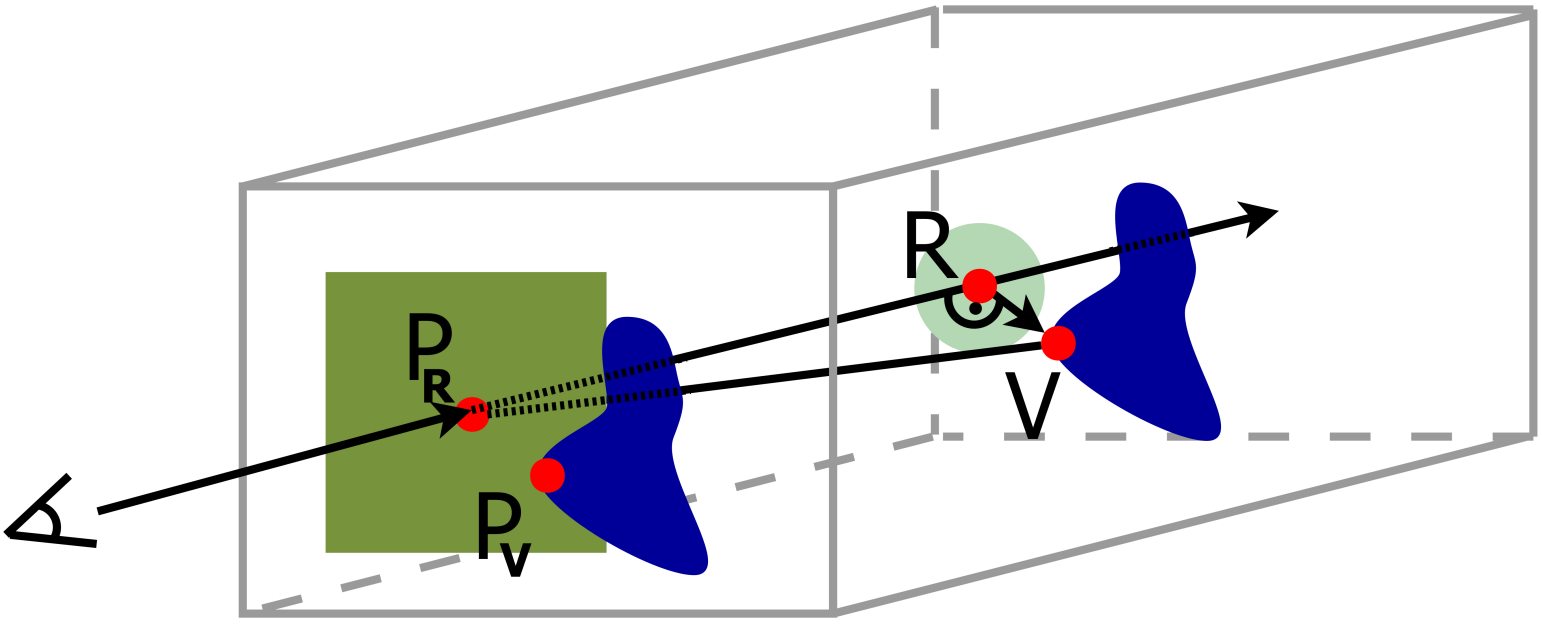

Figure 6.JPEG

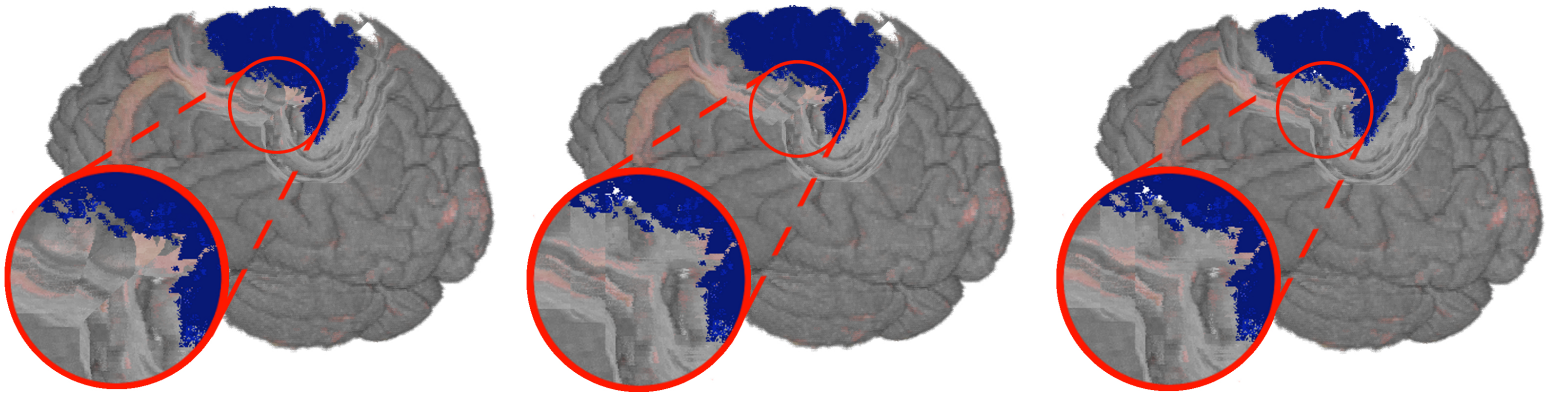

Figure 7.JPEG